

See discussions, stats, and author profiles for this publication at: <https://www.researchgate.net/publication/231707584>

Strengthening Polymer Interfaces with Triblock Copolymers

ARTICLE *in* MACROMOLECULES · FEBRUARY 1997

Impact Factor: 5.8 · DOI: 10.1021/ma960396s

CITATIONS

37

READS

21

7 AUTHORS, INCLUDING:



Raghavachari Dhamodharan

Indian Institute of Technology Madras

100 PUBLICATIONS 1,116 CITATIONS

SEE PROFILE

Strengthening Polymer Interfaces with Triblock Copolymers

Chi-An Dai,[†] Klaus D. Jandt,[‡] Dhamodharan R. Iyengar,[§] Nelle L. Slack,^{||} Kevin H. Dai,[⊥] William B. Davidson, and Edward J. Kramer*

Department of Materials Science and Engineering and the Materials Science Center, Cornell University, Ithaca, New York 14853

Chung-Yuen Hui

Department of Theoretical and Applied Mechanics and the Materials Science Center, Cornell University, Ithaca, New York 14853

Received March 14, 1996; Revised Manuscript Received August 9, 1996[®]

ABSTRACT: We have measured the fracture toughness, G_c , of an interface between polystyrene (PS) and poly (2-vinylpyridine) (PVP) reinforced with triblock copolymers (PVP-*b*-dPS-*b*-PVP) as a function of the areal chain density, Σ , of the copolymers at the interface. The failure mechanisms of the interface are studied by transmission electron microscopy and forward recoil spectrometry. For triblock copolymers with long PVP blocks ($N_{\text{PVP}} > N_{\text{ePVP}}$, where N_{ePVP} is the entanglement polymerization index of PVP), a transition from chain scission at low Σ to crazing at high Σ^* is observed. By comparing the areal chain density Σ^* for the transition from chain scission to crazing for the triblock copolymers ($\Sigma^* = 0.015$ chains/nm²) to that for the diblock copolymers, PVP-dPS ($\Sigma^* = 0.03$ chains/nm²), we show that most of the triblock copolymers form a "staple" structure at the interface with the dPS block making a loop on the PS side of the interface and the PVP ends anchoring the "staple" in the PVP side. As a result of the "staple" structure, the saturation areal chain density of the triblock copolymer (Σ_{sat}) at the interface is half of that for the diblock copolymer of similar molecular weight. For $\Sigma < \Sigma_{\text{sat}}$ in the crazing regime, the fracture toughness of the interface is controlled by the areal joint density, Σ_{cross} , where Σ_{cross} is the number density of the copolymer excursions across the interface. For $\Sigma > \Sigma_{\text{sat}}$, the triblock copolymers appear to reinforce the craze fibrils at the crack tip better than the corresponding diblock copolymers, leading to an interface fracture toughness approaching that of the PS homopolymer itself. For a triblock copolymer with short PVP blocks ($N_{\text{PVP}} < N_{\text{ePVP}}$), there is a transition in the fracture mechanism from pull out of the PVP block to crazing with increasing Σ . Short triblock copolymers can form two chain conformations: one in which two PVP blocks anchor the copolymer on the homopolymer PVP side (staple structure) and one in which one PVP block anchors the copolymer on the PVP side (tail structure) of the interface. Comparison of G_c between the triblock copolymer and the corresponding diblock copolymer is made. The larger G_c values of the triblock copolymer reinforced interface in the crazing regime are observed as a result of enhancement in entanglements between the dPS loops of the triblock copolymer and the homopolymer PS.

Introduction

Interfacial adhesion plays an important role in many industrial applications, e.g. in polymer alloys and polymer coatings, because the interface frequently exerts a limiting effect upon the bulk properties of the material. The addition of diblock copolymers to the interface between immiscible glassy homopolymers has been shown to improve the fracture properties of two-phase polymer mixtures.^{1–3} The increase in mechanical strength is partially due to the ability of the diblock copolymer to act as a polymeric surfactant, segregating to the interface between the immiscible polymers and decreasing the interfacial tension. However, the improvement is mainly due to the ability of the diblock copolymer to form a junction across the interface through which stress can be transferred. The entangle-

ment of the diblock copolymer with its respective homopolymer is now well-established as the mechanism of anchoring that permits such stress transfer.

The mechanism by which the interface fails depends primarily on the areal chain density (number of chains per unit area), Σ , of the diblock copolymer at the interface and the polymerization indices of each block. Mechanisms of failure near crack tip include chain pull out, where one of the blocks of the copolymer chain pulls out from the surrounding homopolymer, and chain scission, where the block copolymer chain actually breaks, usually near the joint in the block copolymer, before any large scale plastic deformation of the homopolymers occurs. Fracture can also occur by crazing of one of the homopolymers followed by failure of the craze by either chain disentanglement or chain scission or a mixture of these two mechanisms in the craze fibrils. Several theoretical models have been proposed to predict the mode of failure of interfaces reinforced with diblock copolymers. Brown² and Hui *et al.*⁴ investigate the mechanics of craze breakdown in glassy polymers and Xu *et al.*⁵ study the crack growth along the interface in the chain pull out regime. Good agreement is found between prediction of the models and the experiments in their respective regimes. Xu *et al.* also introduce a fracture mechanism map that shows which mechanism will dominate according to the level of stress applied to the interface and the areal chain density of block copolymer at the interface.⁵ In

* To whom correspondence should be addressed.

[†] Current address: Manufacturing Research & Engineering Organization, Materials Science and Engineering Division, Eastman Kodak Co., Rochester, NY 14652-3701.[‡] Current address: Department of Oral and Dental Science, Dental Materials and Biomaterials Group, University of Bristol, Lower Maudlin Street, Bristol, BS1 2LY United Kingdom.[§] Current address: Department of Chemistry, India Institute of Technology at Madras, Madras, India.^{||} Current address: Materials Department, University of California at Santa Barbara, Santa Barbara, CA 93106.[⊥] Current address: Corporate Research and Development, General Electric, P. O. Box 8, Schenectady, NY 12301.[®] Abstract published in *Advance ACS Abstracts*, November 15, 1996.

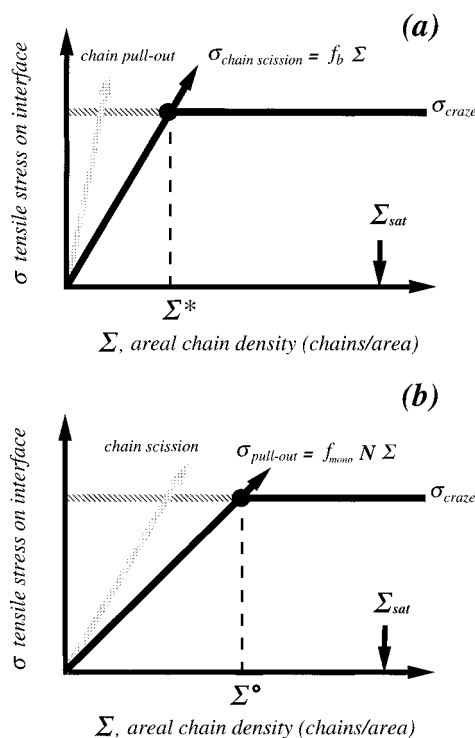


Figure 1. Fracture mechanism map. The tensile stress on the interface, σ , is plotted versus the areal chain density, Σ , of copolymer chains. There are two possible fracture mechanism transitions, depending on the magnitude of $\sigma_{pull\ out}$: (a) for $\sigma_{scission} < \sigma_{pull\ out}$, the interface fails by chain scission for $\Sigma < \Sigma^*$ and by crazing for $\Sigma > \Sigma^*$; (b) for $\sigma_{scission} > \sigma_{pull\ out}$, the interface fails by chain pull out for $\Sigma > \Sigma^\circ$ and by crazing for $\Sigma < \Sigma^\circ$.

this map, shown in Figure 1 a,b, the tensile stress ahead of the crack tip, σ , is plotted as a function of Σ of the copolymer chains at the interface for each failure mechanism. The horizontal line, $\sigma = \sigma_{craze}$, where σ_{craze} is the crazing stress of one of the polymer phase, represents an upper stress limit that is independent of Σ . The vertical arrow, $\Sigma = \Sigma_{sat}$, corresponds to the saturation areal chain density of block copolymer at the interface. For $\Sigma > \Sigma_{sat}$, block copolymers can no longer organize as a brush at the interface but form other microphases, such as micelles or lamellae, near the interface. Chain scission and chain pull out are represented by two lines through the origin, $\sigma_{scission}$ and $\sigma_{pull\ out}$, respectively. The slopes of the chain scission line and chain pull out line represent the forces necessary to break one copolymer or pull it out, respectively. The areal chain densities where the chain scission or chain pull out lines cross the crazing stress correspond to transitions to crazing from chain scission or chain pull out, respectively, as Σ is increased.

At small Σ , the bond-breaking stress, $\sigma_{scission}$, increases linearly with increasing Σ . Since diblock copolymer chains form a brush structure at the interface with only one junction across the interface per chain, the bond-breaking stress of block copolymer chains is given by eq 1:

$$\sigma_{scission} = f_b \Sigma \quad (1)$$

where f_b is the force to break a single carbon-carbon bond. The stress required to cause chain pull out, $\sigma_{pull\ out}$ is dependent on the frictional forces at work between the homopolymer matrix and the copolymer block being pulled-out and is assumed to be given by

$$\sigma_{pull\ out} = f_{mono} N \Sigma \quad (2)$$

where f_{mono} denotes a static friction coefficient per monomer and N is the polymerization index of the block subjected to pull out.

Depending on the value of N , a different failure mechanism will result. The dominant mechanism will be that which requires the lowest stress. For $N_{PVP} \gg N_{ePVP}$, chain scission requires lower stress than chain pull out and the interface fails by chain scission for $\Sigma < \Sigma^*$, as shown in Figure 1a. The interfacial stress continues to increase until the stress is high enough to plastically deform one of homopolymers by crazing. At this point Σ is equal to Σ^* , where Σ^* is the areal density at transition from chain scission to crazing. For $\Sigma > \Sigma^*$, crazing occurs on the PS side of the interface and the interfacial stress, σ , remains constant and is equal to σ_{craze} . For $N_{PVP} < N_{ePVP}$, the chain pull out line may have a smaller slope than the chain scission line and the chain pull out mechanism will be active at small Σ , as shown in Figure 1b. Crazing will dominate chain pull out when Σ is greater than a critical value, Σ° , where Σ° is the areal density at transition from chain pull out to crazing. For $\Sigma < \Sigma^\circ$, the interface fails by chain pull out, while for $\Sigma > \Sigma^\circ$ the interface fails by crazing. For N_{PVP} appreciably smaller than N_{ePVP} , the interface may become saturated (Σ_{sat}) with the block copolymer before Σ° is reached and no pull out to crazing transition will be possible.

The system we have chosen consists of the immiscible homopolymers polystyrene (PS) and poly(2-vinylpyridine) (PVP). Both homopolymers deform predominately by crazing; however, PS has a smaller crazing stress than PVP (≈ 55 MPa for PS and ≈ 75 MPa for PVP).³ The interface is reinforced with poly(2-vinylpyridine)-*b*-deuterated-polystyrene-*b*-poly(2-vinylpyridine) (PVP-*b*-dPS-*b*-PVP) triblock copolymers. Many studies have been done to investigate the strengthening effect of the interfaces between immiscible polymers reinforced with diblock copolymers and more recently with random copolymers.⁶⁻¹⁰ The objective of this work is to explore the difference in the fracture properties of the interfaces reinforced with diblock copolymers and triblock copolymers. In addition, this study may provide some understanding of the chain conformation and the microstructure of the triblock copolymer at the interface.

Experimental Section

1. Materials. PS and PVP homopolymers were purchased from Aldrich Chemical Co. and Polysciences, Inc., respectively and had weight-average molecular weights of 270 000 ($\bar{M}_w/\bar{M}_n \approx 2.1$) and 250,000 ($\bar{M}_w/\bar{M}_n \approx 2.4$), respectively. Diblock copolymers (PVP-*b*-dPS) and triblock copolymers (PVP-*b*-dPS-*b*-PVP) were synthesized via living anionic polymerization. The polymerization consists of a two-stage sequential addition of deuterated styrene and 2-vinylpyridine monomers into tetrahydrofuran solvent at -55°C in an argon atmosphere. The reaction was carried out using cumylpotassium as monofunctional initiator for the diblock copolymers and using (α -methylstyryl)potassium as the difunctional initiator for the triblock copolymers.¹¹ At the end of each stage, aliquots were taken to recover the dPS precursor and the block copolymer, respectively, for later characterization. The molecular weight and composition of these block copolymers were measured by gel permeation chromatography (GPC) and forward recoil spectrometry (FRES) and are listed in Table 1. The triblock copolymer consisting of a PS block with a degree of polymerization (DP) of 1620 and two PVP end blocks with a DP of 580 will be designated as 580-1620-580. For comparison, the diblock copolymer whose DP of the PVP block is 870 and that

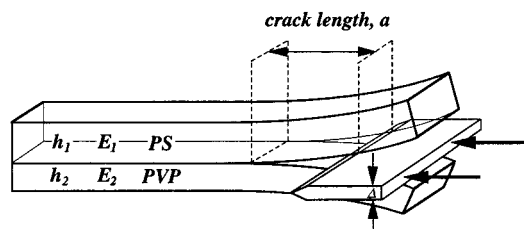


Figure 2. Schematic of asymmetric double cantilever beam sample for the fracture toughness test.

Table 1. Polymerization Index of the Triblock and the Diblock Copolymers

triblock copolymers, PVP- <i>b</i> -dPS- <i>b</i> -PVP	diblock copolymers, PVP- <i>b</i> -dPS
580–1620–580	870–800
290–470–290	540–510
90–570–90	220–580

of the dPS block is 800 will be denoted as 870–800. The triblock copolymers PVP-*b*-dPS-*b*-PVP 580–1620–580 and 290–470–290 and the diblock copolymers PVP-*b*-dPS 870–800 and 540–510 have polymerization indices for both blocks higher than the polymerization index between entanglements, N_e , of their respective homopolymer ($N_{ePS} \approx 173$, $N_{ePVP} \approx 255$). For the 90–570–90 and 220–580, the PVP blocks of the copolymers cannot form entanglements with PVP homopolymer since their PVP blocks are too short. The polystyrene blocks of the copolymers were deuterated in order to allow for their use as labels in the subsequent FRES experiments. The FRES technique utilizes a ^4He ion beam impinging on an area $\sim 5 \text{ mm} \times 1 \text{ mm}$ of each fracture surface of the sample.¹² The energy of recoiled hydrogen and deuterium particles is recorded and converted into a depth scale based on the energy loss of the particles on their path through the sample. The amount of deuterium averaged over the probe area on each fracture surface is determined by integrating its spectrum signal in FRES, which is readily converted into an apparent areal chain density, Σ , of the deuterated PS block of the copolymer on each side of the fracture ($\Sigma(\text{PS})$ and $\Sigma(\text{PVP})$). The total areal chain density is then given by $\Sigma = \Sigma(\text{PS}) + \Sigma(\text{PVP})$.

2. Sample Preparation. Plates of polydisperse PS and PVP with dimension of $5 \text{ cm} \times 7 \text{ cm} \times 2.4 \text{ mm}$ and $5 \text{ cm} \times 7 \text{ cm} \times 1.7 \text{ mm}$, respectively, were made by compression molding at 160°C . A thin film of the block copolymer was spun cast from a toluene solution onto the PVP plate. The thickness of the copolymer film or the areal chain density, Σ , of the copolymer is controlled by the concentration of the copolymer solution that is spun onto the PVP plate. The homopolymer PS plate is welded to the copolymer-coated PVP plate to form a PS/copolymer/PVP assembly by annealing at 160°C for 2 h. The final PS/copolymer/PVP sandwiches were cut into eight strips for the fracture toughness measurements.

3. Fracture Toughness Measurement. The interfacial fracture toughness, or the critical energy release rate, G_c , is measured using the asymmetric double cantilever beam method (ADCB). A schematic drawing of this method is shown in Figure 2. A razor blade of known thickness, Δ , is inserted into the PS/PVP interface. A crack is initiated ahead of the edge of the razor blade. This razor blade is then driven by a servo motor at a constant speed ($3 \times 10^{-6} \text{ m/s}$). Steady state crack propagation was established after several minutes. The entire history of crack progression, in particular the length (a) of the crack ahead of the razor blade, is recorded using a video camera so that many measurements of a could be made using one PS/copolymer/PVP strip. The error bars reported subsequently for G_c represent one standard deviation of at least 16 crack length measurements. The crack length a is converted to G_c using the relation first developed by Kanninen¹³ and later modified by Creton *et al.*,³ i.e.

$$G_c = \frac{3\Delta^2}{8a^4} (E_1 E_2 h_1^3 h_2^3) \frac{(C_1^2 E_2 h_2^3 + C_2^2 E_1 h_1^3)}{(C_1^3 E_2 h_2^3 + C_2^3 E_1 h_1^3)^2} \quad (3)$$

where $C_1 = 1 + 0.64h_1/a$ and $C_2 = 1 + 0.64h_2/a$. E_1 and E_2 are the Young's moduli, and h_1 and h_2 are the thickness of PS and PVP homopolymer beams, respectively.

It should be noted that, as a crack propagates along a interface between two materials with different elastic moduli, the stress field of the crack tip along the interface in general has both tensile (mode I) and shear (mode II) components. A phase angle, Ψ , is defined as a measure of the relative shear to the opening components. To assure that the crack propagates at the PS/PVP interface, the plate of the more compliant material (PS) is made to be thicker than the PVP plate, giving rise to a mechanical phase angle $\Psi \approx -6^\circ$. At this value of Ψ , the fracture toughness of the interface is a minimum and is only weakly dependent on Ψ as long as $\Psi < 0$. A detailed discussion of the effects of Ψ on the fracture of PS/PVP interfaces reinforced with diblock copolymers is available elsewhere.¹⁴

4. TEM Observation of Interface Structure. Cross-sectional transmission electron microscopy (TEM) was used to investigate the structure of the interfaces reinforced with diblock copolymers¹⁵ and triblock copolymers. A small piece of the PS/copolymer/PVP strip was partially embedded in an epoxy resin that was then cured at room temperature to provide a sample that would be suitable for microtoming. Thin sections ($\sim 100 \text{ nm}$ thick) were cut from the sample strip with a microtome using a glass knife at room temperature. The microtomed film was transferred to the surface of a water bath. Wrinkles in the film induced by the cutting process were removed by exposing the film briefly to a mixed solvent vapor (toluene/chloroform = 50/50). This step did not result in noticeable changes in the interfacial structure. The film was subsequently picked up onto a gold grid and dried in vacuum. The film was then exposed to iodine vapor for 12 h to selectively stain the PVP phase. The staining enhances the electron scattering from the PVP phase and leads to a distinguishably "darkened" PVP phase under TEM. A JEOL 1200EX TEM operating at 120 keV was used for the TEM observations.

Results and Discussion

A. Long Triblock Copolymers (N_{PVP} above N_{ePVP}). 1. Chain Scission to Crazing Transition.

Figure 3a shows the fracture toughness of the PS/PVP interface reinforced by the triblock copolymer 580–1620–580 PVP-*b*-dPS-*b*-PVP as a function of its areal chain density, Σ . At small Σ , G_c increases roughly linearly with increasing Σ . Note that G_c is low until a critical value of $\Sigma > \Sigma_{tri}^* \approx 0.015 \text{ chains/nm}^2$ is exceeded and then it increases strongly and reaches a value around 150 J/m^2 for $\Sigma \approx 0.1 \text{ chains/nm}^2$. In Figure 3b, the fraction of deuterium (or dPS) found on the PS fracture surface, $\Sigma(\text{PS})/\Sigma$, is plotted vs Σ . For the 580–1620–580 triblock copolymer nearly 90% of the dPS is found on the PS side of the fracture up to a $\Sigma = 0.015 \text{ chains/nm}^2$, at which point a transition occurs and the value of $\Sigma(\text{PS})/\Sigma$ starts to decrease with increasing Σ , eventually achieving a value of ~ 0 –10% of the dPS on the PS side of the fracture for $\Sigma \approx 0.1 \text{ chains/nm}^2$. This observed transition suggests that the locus of fracture changes from the region of the PS/PVP interface to the region of the interface between the dPS block and the PS homopolymer when Σ is increased above $\Sigma_{tri}^* \approx 0.015 \text{ chains/nm}^2$. The larger G_c values are indicative of plastic deformation ahead of the crack tip near the interface region. Optical microscopy of the fracture surfaces was used to verify that a wide craze does not form on the PS side for $\Sigma < \Sigma_{tri}^*$ and does form for $\Sigma > \Sigma_{tri}^*$.

The large increase in the measured G_c above the transition as well as the change in the locus of fracture suggests a change in fracture mechanism with increasing Σ . For PS/PVP interfaces reinforced with a long

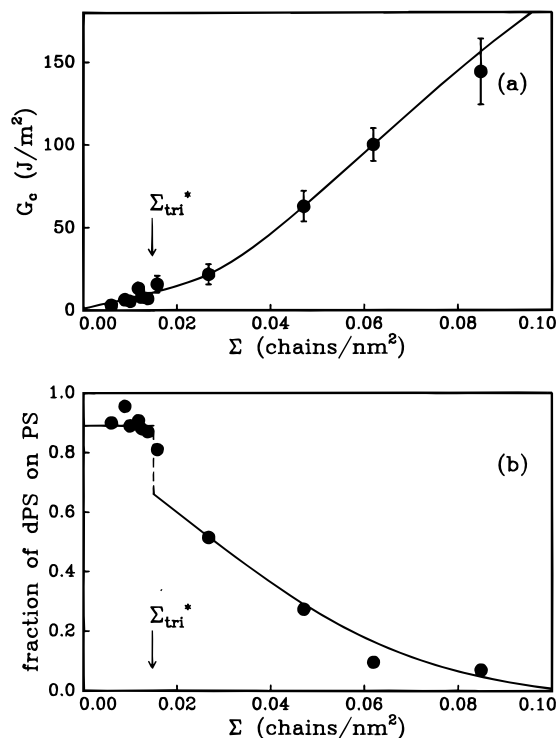


Figure 3. (a) Fracture toughness, G_c , plotted versus the areal chain density, Σ , of the 580–1620–580 triblock copolymer. (b) Fraction of the dPS found on the PS fracture surface plotted versus Σ .

diblock copolymer, Creton *et al.*³ show that there is a fracture transition from chain scission of diblock copolymers to crazing of PS homopolymer with a transition value of $\Sigma_{di}^* = 0.03$ chains/nm². From the fracture mechanism map shown in Figure 1, at the chain scission to crazing transition, the interfacial stress, σ , is given by

$$\sigma = f_b \Sigma_{di}^* = \sigma_{craze} \quad (4)$$

Equation 4 can be confirmed by estimating the bond breaking force of a carbon–carbon bond (f_b) from the measurement of Σ_{di}^* and σ_{craze} . Creton *et al.* derived an estimate of $f_b \approx 2 \times 10^{-9}$ N, in good agreement with other experimental studies^{2,16} and theoretical predictions.¹⁷

The same kind of fracture transition from chain scission (without crazing) to crazing followed by craze failure is observed for the 580–1620–580 triblock copolymer. However, the transition areal chain density for the triblock copolymer (0.015 chains/nm²) is just half that of the diblock copolymer. Since the breaking force, f_b , for a bond in the triblock copolymer chain must be the same as that in the diblock copolymer, it must be necessary to break two bonds in each triblock copolymer chain where the interface fails by chain scission. The logical conclusion is that the triblock copolymers form a hairpin or a “staple” structure at the interface with the dPS block forming a loop on the PS side of the interface and the PVP ends anchoring the “staple” in the PVP side. A schematic drawing of chain conformation of the triblock copolymer at the interface is shown in Figure 4a.

It should be pointed out that the transition areal chain density from chain scission to crazing with increasing Σ is characteristic of the PS/PVP polymer interface and is independent of the details of the “connector chains” (e.g. molecular weight of block co-

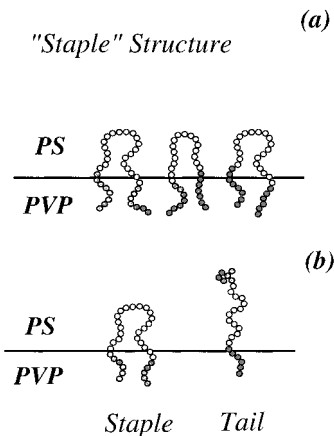


Figure 4. (a) Schematic representation of the staple structure of the long triblock copolymer at the interface. (b) Schematic representation of the staple and the tail conformations of a short triblock copolymer at the interface.

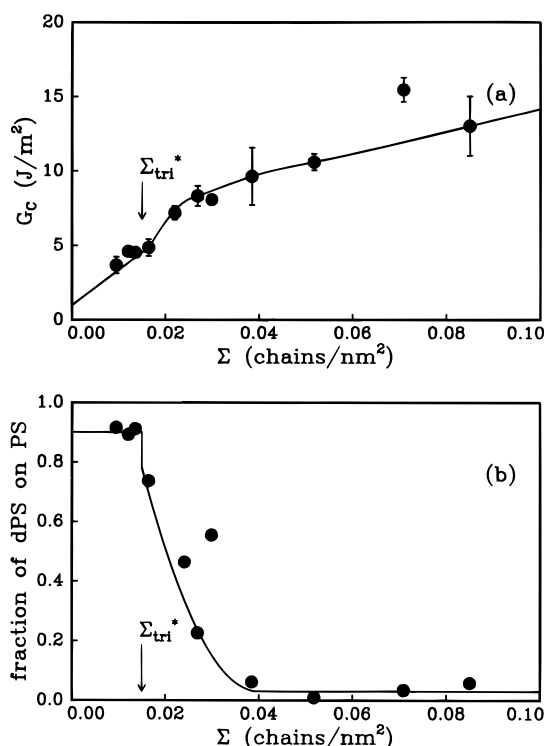


Figure 5. (a) Fracture toughness, G_c , plotted versus the areal chain density, Σ , of the 290–470–290 triblock copolymer. (b) Fraction of the dPS found on the PS fracture surface plotted versus Σ .

polymer) as long as these are well-anchored on each side of the interface. For the interface reinforced with the triblock copolymer 290–470–290, as shown in Figure 5a, G_c increases approximately linearly with increasing Σ until the same critical Σ ($\Sigma \approx \Sigma_{tri}^* = 0.015$ chains/nm²) is reached. There is a slight change in slope of the G_c vs Σ curve for $\Sigma > \Sigma_{tri}^*$. For $\Sigma \leq 0.1$ chains/nm², the maximum G_c value is only about 15 J/m². Figure 5b shows that $\Sigma(\text{PS})/\Sigma$ decreases abruptly from ~ 0.9 for $\Sigma < \Sigma_{tri}^*$ to ~ 0.05 for $\Sigma > \Sigma_{tri}^* = 0.015$ chains/nm². Thus there is also a transition from chain scission to crazing for the interface reinforced with the 290–470–290 triblock copolymer at the same value $\Sigma_{tri}^* = 0.015$ chains/nm² as for the 580–1620–580 triblock copolymer. Therefore, we infer that the 290–470–290 triblock copolymer also forms a staple structure at the interface.

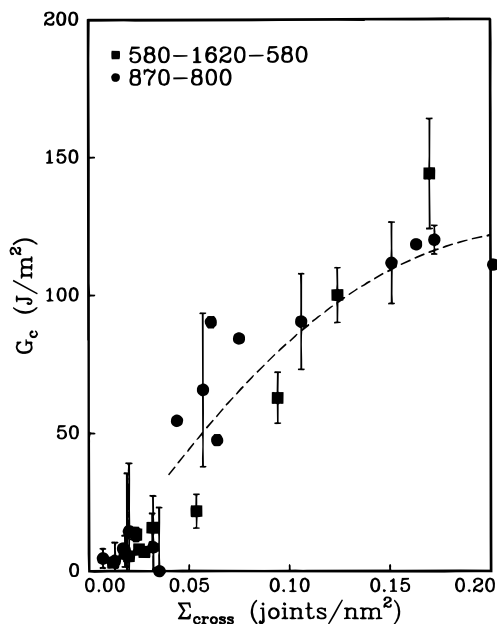


Figure 6. Plot of fracture toughness, G_c , plotted versus the areal chain density of chain crossing, Σ_{cross} , of the 580–1620–580 triblock copolymer (■) and the 870–800 diblock copolymer (●).

2. Crazing Fracture at Medium Areal Chain Density ($\Sigma \leq 0.1$ chains/nm²). On the basis of the hairpin morphology of the triblock copolymer at the interface, one can assume, as a first approximation, that a triblock copolymer effectively consists of two “pseudodiblock” copolymers. The assignment for the effective degree of polymerization (DP) of each block of the pseudodiblock copolymer is as follows: the DP of the dPS block of the pseudodiblock copolymer is equal to half of that of the dPS block of the triblock copolymer, and the DP of the PVP block of the pseudodiblock copolymer is equal to that of the PVP block of the triblock copolymer. We can also define a new areal density, Σ_{cross} , the areal joint density, which is the number density of the copolymer excursions across the interface. The areal joint density of a diblock copolymer which crosses the interface only once is equal to its areal chain density, Σ , while that of a long triblock copolymer is equal to 2Σ , if the triblock copolymer adopts the staple configuration.

We can test the above assumption by comparing the fracture toughness (G_c) of the PS/PVP interface as a function of areal joint density (Σ_{cross}) of the triblock copolymer 580–1620–580 PVP-*b*-dPS-*b*-PVP with that of the diblock copolymer 870–800 PVP-*b*-dPS in Figure 6. Note that the DP of the dPS in the diblock copolymer is only half of that of the dPS in the triblock copolymer chain. It is clear from the data that the G_c values are roughly the same for the triblock copolymer and the diblock copolymer for the same areal joint density up to 0.2 joints/nm². Thus, at least at areal chain densities too low for separate block copolymer mesophases to form adjacent to the interface, the areal joint density (Σ_{cross}) seems to be the parameter that controls the G_c of the interface under conditions where a craze forms in the PS adjacent to the interface.

Another example to test whether Σ_{cross} controls G_c is shown in Figure 7. In this case G_c vs Σ_{cross} is plotted for the triblock copolymer 290–470–290 PVP-*b*-dPS-*b*-PVP and the diblock copolymer 540–510 PVP-*b*-dPS. Note that the dPS block of both copolymers has roughly the same degree of polymerization. For $\Sigma_{\text{cross}} \leq 0.2$

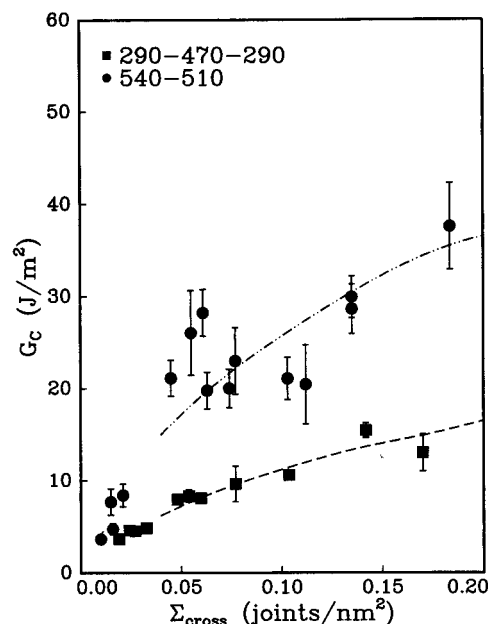


Figure 7. Plot of fracture toughness, G_c , plotted versus the areal chain density of chain crossing Σ_{cross} , of the 290–470–290 triblock copolymer (■) and the 540–510 diblock copolymer (●).

joints/nm², the measured fracture toughness of the interface reinforced with the diblock copolymer is always larger than that of the interface reinforced with the triblock copolymer in the crazing regime. The G_c value for the diblock copolymer increases with increasing Σ_{cross} , but the G_c value for the triblock copolymer hardly increases at all with increasing Σ_{cross} . This comparison, however, is not between the triblock copolymer and its corresponding pseudodiblock copolymer but rather with a diblock copolymer for which the dPS block is more than twice as long. The DP of the dPS block of the pseudodiblock copolymer is about $470/2 = 235$ which is only slightly larger than that of entanglement of homopolymer PS ($N_{\text{ePS}} \approx 173$) and is much smaller than the DP of the dPS block of the 540–510 diblock copolymer. A wide craze cannot be formed at the interface since the dPS loop of the triblock copolymer is only marginally entangled with the homopolymer PS and the load-bearing capability of the craze fibrils adjacent to the interface is thus relatively low.

3. Crazing Fracture at High Areal Chain Density ($\Sigma \geq 0.1$ chains/nm²). (a) G_c Measurement. Parts a and b of Figure 8 show G_c as a function of Σ up to $\Sigma \approx 1.0$ chains/nm² for the 290–470–290 and the 580–1620–580 triblock copolymers, respectively. For the 290–470–290 triblock copolymer, G_c hardly increases with increasing Σ for $\Sigma \leq 0.15$ chains/nm². However, G_c increases rapidly for $0.15 \leq \Sigma \leq 0.2$ chains/nm² and then reaches a constant value of around 80 J/m² for $\Sigma \geq 0.2$ chains/nm². For the 580–1620–580 triblock copolymer, G_c increases strongly for $\Sigma \leq 0.2$ chains/nm² and finally reaches a value of ~ 330 J/m² for $\Sigma \geq 0.2$ chains/nm².

The results show that the G_c values saturate for the interfaces reinforced with long nearly symmetric triblock copolymers at large Σ (for $\Sigma \geq 0.2$ chains/nm²). In contrast, several studies show that there is an optimum Σ for reinforcing the interface with symmetric diblock copolymers.^{8,9,18} Results for the 540–510 and 870–800 PVP-dPS diblock copolymers are reproduced in Figure 8c,d for comparison.⁸ In order to investigate the reason

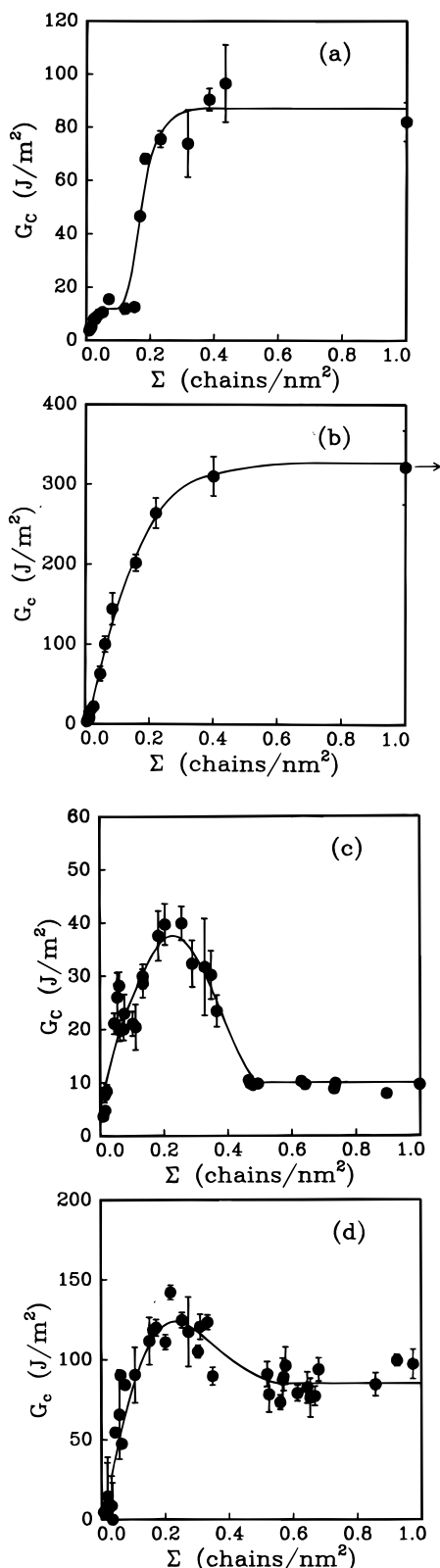


Figure 8. Fracture toughness, G_c , plotted as a function of areal chain density, Σ , of the triblock and diblock copolymers. The interfaces are reinforced with (a) the 290–470–290 triblock copolymer, (b) the 580–1620–580 triblock copolymer, (c) the 540–510 diblock copolymer (data of Washiyama *et al.*⁸) and (d) the 870–800 diblock copolymer (data of Washiyama *et al.*⁸).

for such G_c behavior in more detail, a closer examination of the interface microstructure is necessary.

(b) TEM Analysis of the Interface. Figure 9a–f shows TEM micrographs of the PS/PVP interfacial

microstructure for $\Sigma \approx 0.09, 0.17, 0.2, 0.4, 0.6$, and 1.0 chains/nm², respectively, of 290–470–290 triblock copolymer. Figure 9a shows that there is a distinct interface that separates PS (bright) and PVP (dark) phases, indicating that the interface is not saturated with triblock copolymers yet at $\Sigma \approx 0.09$ chains/nm². As Σ increases to $\Sigma = 0.17$ chains/nm², lamellae of finite size (lamellar islands) of the triblock copolymer are seen at the interface in Figure 9b. We define one lamella as one PS sublamella and one PVP sublamella. For $\Sigma \approx 0.2$ chains/nm², a region where a well-organized full coverage of the first lamella parallel to the interface is seen in Figure 9c. At larger Σ ($\Sigma \approx 0.4$ chains/nm²), a second lamella covers the whole interface as shown in Figure 9d. Although regions of fully organized lamellar structure parallel to the interface can be seen occasionally near the interface, we found that the lamellar structure is generally not uniform along the interface, as illustrated by the structure shown in Figure 10. The figure shows a dislocation-like defect of the lamellar structure along the interface for $\Sigma \approx 0.22$ chains/nm² as measured by FRES. At even larger Σ ($\Sigma > 0.6$ chains/nm²) the lamellae become disordered as shown in Figure 9e,f. At these large values of Σ , long-range ordered lamellae that are parallel to the interface are rarely seen. The nonuniformity of lamellae formed at the interface may be due to several reasons. Triblock copolymers may form a so-called “mesogel”^{19,20} in the concentrated solutions necessary to produce thick layers. As a result, the spin-casting of such triblock copolymer solutions does not produce uniform thin films at the interface. In addition, the multiple lamellae of the triblock copolymer may need a longer annealing time than 2 h to organize themselves completely.

We compare the thickness (spacing of one complete PS and PVP sublamella) of the lamella of triblock copolymer 290–470–290 to that of the diblock copolymer 510–540 in Figure 11a,b. The thickness of lamella for the triblock copolymer (~ 33 nm) is only about half of that for the similar molecular weight diblock copolymer (~ 70 nm).²¹ Earlier work on comparing lamellar spacing between diblock copolymers and triblock copolymers also found similar results.²² For a symmetric block copolymer, the largest possible areal density of chains crossing the interface Σ_{sat} will be the areal density in the lamellar microdomains of the corresponding pure block copolymer,

$$\Sigma_{\text{sat}} = \frac{1}{4} \frac{\rho_m L}{N} \quad (5)$$

where ρ_m is the number of monomer per unit volume, N is the DP of each block, and L is the lamellar thickness. Since the 540–510 diblock copolymer and 290–470–290 triblock copolymer have the same total molecular weight, Σ_{sat} for the lamella of the triblock copolymer is only about half of that for the lamella of the diblock copolymer from eq 5. Washiyama *et al.* show that the interface reinforced with diblock copolymer is saturated with diblock copolymers at $\Sigma \approx \Sigma_{\text{sat}} = 0.2$ chains/nm². Therefore, for the triblock copolymer with the same molecular weight as the diblock copolymer, the interface will be saturated with triblock copolymers at $\Sigma \approx \Sigma_{\text{sat}} = 0.1$ chains/nm². The information on lamella thickness for diblock copolymers and triblock copolymers is also consistent with the chain conformations of diblock copolymers and triblock copolymers in a lamella. As shown in Figure 12a,b, diblock copolymers that form polymer brushes in the lamella repel each

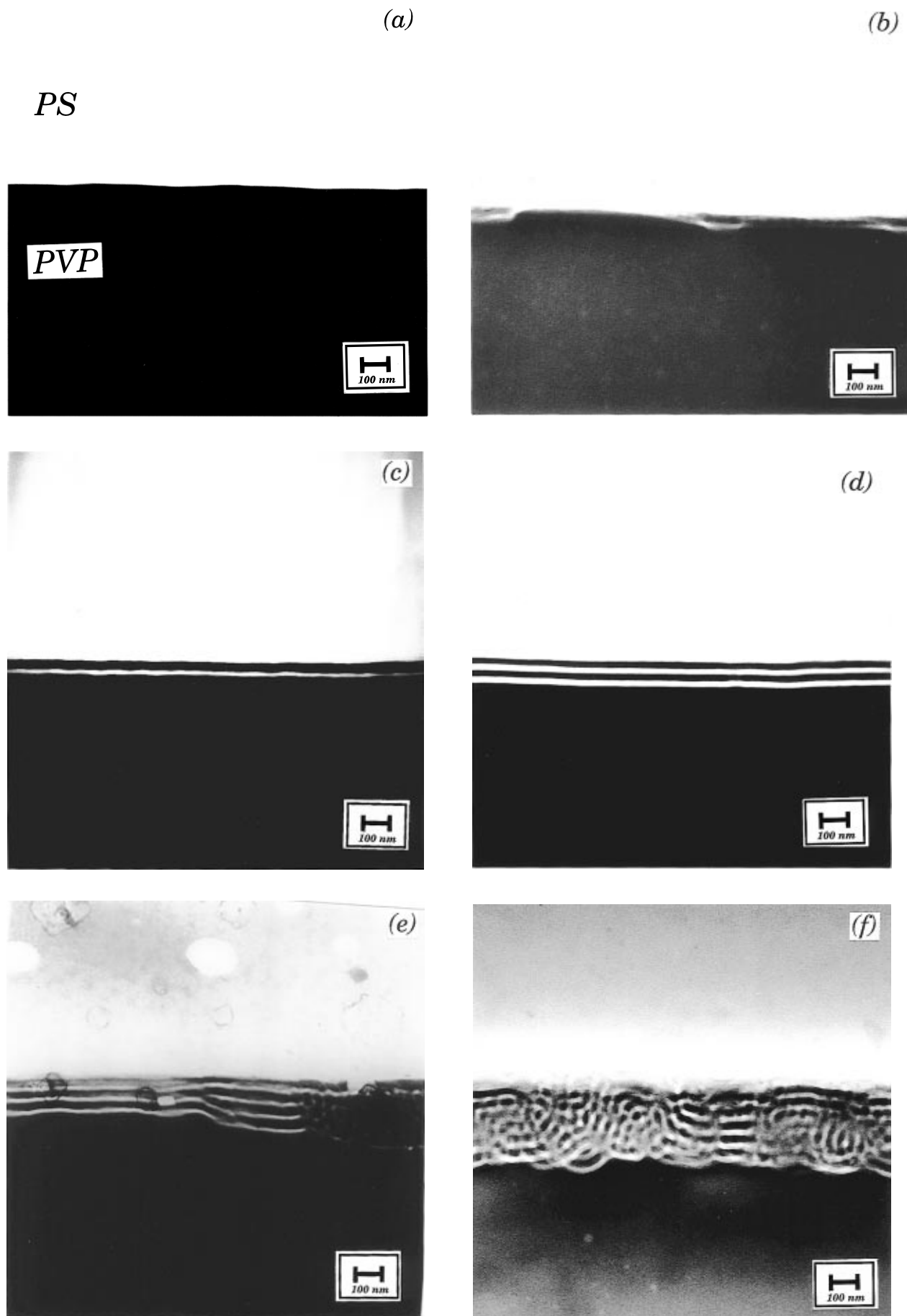


Figure 9. TEM micrographs of the morphology of the 290–470–290 triblock copolymer microstructure near the interface for (a) $\Sigma = 0.09$, (b) $\Sigma = 0.17$, (c) $\Sigma = 0.22$, (d) $\Sigma = 0.4$, (e) $\Sigma = 0.6$, (f) $\Sigma = 1.0$ chains/nm². In the micrographs, the PS phase appears to be bright and PVP phase appears to be dark due to the staining process. Note that disordered lamellae are found for $\Sigma > 0.6$ chains/nm².

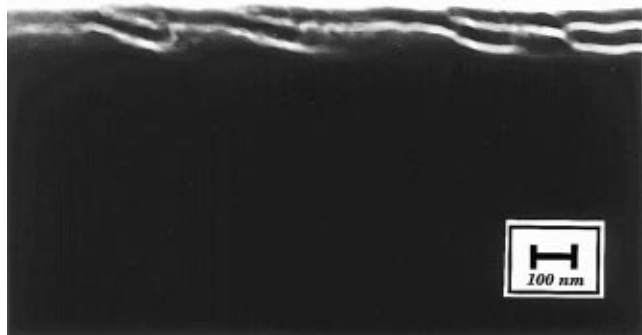


Figure 10. TEM micrograph of the irregular lamellar structure of the 290-470-290 triblock copolymer along the interface for an average areal chain density $\Sigma = 0.22$ chains/nm².

other from the neighboring subdomains, while the midblock of triblock copolymers forms both staple and bridging structures in a lamella. In contrast, for the lamellae of diblock copolymers, the midblock lamellae of triblock copolymers contain many bridging chains that directly connect adjacent lamellar layers. The effect of chain connectivity of the triblock copolymer on the G_c will be discussed in detail later.

The interface reinforced with 580-1620-580 triblock copolymer was found to have a different morphology than that with 290-470-290 triblock copolymer at high Σ . Figure 13 a-c shows TEM micrographs of interfacial structure with $\Sigma = 0.1, 0.2$, and > 1.0 chains/nm² of 580-1620-580. As was predicted above, Σ_{sat} for the triblock copolymer is ~ 0.1 chains/nm². Indeed, as shown in Figure 13a, no distinct lamellar or other structure of the triblock copolymer 580-1620-580 was found at the PS/PVP interface for $\Sigma \approx 0.1$ chains/nm². Figure 13b shows that a complete layer of the triblock copolymer microdomain forms near the interface when $\Sigma \approx 0.2$ chains/nm². Figure 13c shows a thicker layer of such structure at larger Σ ($\Sigma > 1.0$ chains/nm²). This triblock copolymer layer appears to consist of interconnected cylinders of PVP (or PVP fingers) in a dPS matrix. The PVP fingers are oriented preferentially perpendicular to the triblock copolymer layer/homopolymer PS and the triblock copolymer layer/homopolymer PVP interfaces. Both interfaces are no longer flat and uniform on a 50 nm scale but are characterized by a roughness caused by the alternation of PVP and PS domains along the interface. The "finger" microstructure of the triblock copolymer layer may account for part of the enhancement of G_c in the large Σ regime for this triblock copolymer compared with its closest equivalent diblock copolymer (the 870-800).

(c) Failure Analysis. Parts a and b of Figure 14 show the areal chain densities of the 290-470-290 and 580-1620-580 triblock copolymers, respectively, found on the PS or the PVP side, $\Sigma(\text{PS})$ and $\Sigma(\text{PVP})$, as a function of Σ . Note that $\Sigma = \Sigma(\text{PS}) + \Sigma(\text{PVP})$. Both plots show that $\Sigma(\text{PVP})$ monotonically increases with increasing Σ ($\Sigma(\text{PVP}) \approx \Sigma$) while $\Sigma(\text{PS})$ remains at very low values with increasing Σ . For the 290-470-290 triblock copolymer, $\Sigma(\text{PS})$ has a value of ~ 0.05 chains/nm²,

while for the 580-1620-580 triblock copolymer the average value of $\Sigma(\text{PS})$ is about $\sim 0-0.01$ chains/nm² for $\Sigma \geq \Sigma_{\text{sat}} \approx 0.1$ chains/nm².

Combining the results presented in sections a-c, we can now explain the G_c behavior in the medium and high Σ regime ($\Sigma \geq 0.1$ chains/nm²) for both 290-470-290 and 580-1620-580 triblock copolymer reinforced interfaces. There are large increases in the measured G_c values as the triblock copolymer mesophase forms at the interface for $0.1 \leq \Sigma \leq 0.2$ chains/nm². The fracture toughness levels off for $\Sigma \geq 0.2$ chains/nm². Although a negative phase angle ($\Psi \approx -6^\circ$) coming from the mechanical testing geometry tends to push a craze or a crack tip toward the PVP bulk, the crack tip or craze is not found to penetrate through the triblock copolymer layer due to two possible reasons. First, as discussed earlier, the triblock copolymer layer forms an interconnected microstructure in the dPS domains, and as a result, it would require large amount of energy dissipation for a crack to propagate through this layer. Second, PVP domains of the triblock copolymer layer are craze-resistant since PVP blocks of the copolymer are well-entangled with each other and have a higher crazing stress than the PS.

The chain connectivity in the dPS midblock domains of the triblock copolymer is crucial in allowing a large G_c to be obtained for multilamellar overgrowths on the interface. In the case of the 540-510 diblock copolymer of PVP-*b*-dPS, the lack of this connectivity allows the crack to propagate in the PS sublamella immediately adjacent to the interface. The low fracture toughness of the interface reinforced with multiple layers of the diblock copolymer ($G_c \approx 10$ J/m² for $\Sigma > 0.4$ chains/nm² of the 540-510 diblock copolymer and $G_c \approx 80$ J/m² for $\Sigma > 0.4$ chains/nm² of the 870-800 diblock copolymer as shown in parts c and d of Figure 8, respectively) is a result of this weakness of the dPS sublamella which can craze at nearly the same stress as the homopolymer PS. Such a sublamella craze will allow a crack to grow into it at low interface stresses in the craze fibrils. The weakness of the dPS sublamella of the diblock copolymer is compounding by the fact that it is swollen significantly by the low molecular weight fraction of the polydisperse PS homopolymer.^{8,23} The triblock copolymer layers, on the other hand, are not likely to be swollen significantly by the low molecular weight fraction of the polydisperse PS since if the dPS domains were swollen, the chain connectivity would require significant chain stretching in the dPS domains.

The failure analysis in section c shows that as Σ increases, the locus of fracture is close to the interface between the outer dPS loops of the triblock copolymer mesophase and the homopolymer PS. Thus, we expect that the interfacial microstructure between the triblock copolymer layer and homopolymer PS is important for craze widening and crack tip propagation. As shown in the TEM micrographs in section b, however, the interface between the triblock copolymer layers and the homopolymer PS is not uniform due to the formation of dislocations and disordered lamellae for the 290-470-290 triblock copolymer. The interface between the 580-1620-580 triblock copolymer layer and the homopolymer PS is also not uniform. The outer dPS loops, originating from the tips of the PVP fingers, and which form entanglements with the homopolymer PS, cannot remain at the same plane as the outer dPS domains between two adjacent PVP fingers. A schematic of a crack propagating at the interface is shown in Figure

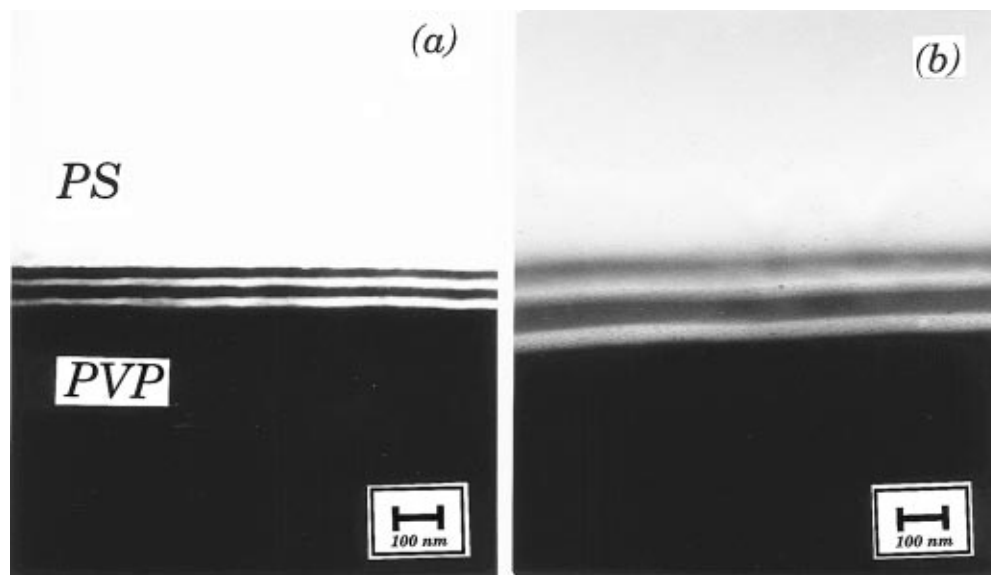


Figure 11. TEM micrographs of lamellar structure of (a) the 290–470–290 triblock copolymer and (b) the 540–510 diblock copolymer near the interface. Note that both of the micrographs have the same magnification. The lamellar spacing is ~ 33 nm for the diblock copolymer and is ~ 70 nm for the triblock copolymer.

15 a,b. A crack must propagate and attempt to trace along the “rough” contour of the interface between the outer triblock copolymer layer and the homopolymer PS since the interface is likely to be weakest there. The requirement for the crack or craze to make excursions away from the PVP interface would dissipate significant amounts of energy. Due to the negative phase angle, the crack may be occasionally forced to penetrate through the homopolymer PS phase (e.g. in the “webs” between the PVP fingers of the 580–1620–580 triblock copolymer) leading to a large increase in the fracture toughness of the interface as the triblock copolymer layer starts to overgrow at the PS/PVP interface.

B. Short Triblock Copolymer (N_{PVP} below N_{ePVP}).

1. Chain Pull Out to Crazeing Transition. Figure 16a shows G_c as a function of Σ for a 90–570–90 triblock copolymer. The measured fracture toughness increases linearly with Σ until a critical $\Sigma_{\text{tri}} = 0.07$ chains/nm², is reached, at which point there is a discontinuous transition as the fracture toughness jumps to a plateau value of approximately 30 J/m². Figure 16b shows that all of the dPS ($\sim 100\%$) is found on the PS side of fractured samples up to $\Sigma = 0.07$ chains/nm², at which point a transition occurs and the value of $\Sigma(\text{PS})/\Sigma$ drops to ~ 0.45 with increasing Σ .

The transition in the G_c versus Σ relationship is characteristic of a transition in the mechanism responsible for fracture. At low Σ , there is a linear relationship between G_c and Σ , and the fracture mechanism is either chain pull out or chain scission. Both mechanisms result in G_c scaling linearly with Σ .³ It is reasonable to assume that the PVP block is being pulled out for $\Sigma < 0.07$ chains/nm², since there are no effective entanglements between the PVP block ($N_{\text{PVP}} < N_{\text{ePVP}}$) and PVP homopolymer. In addition, the FRES evidence ($\Sigma(\text{PS})/\Sigma$) strongly indicates that the interface fails by chain pull out for $\Sigma < \Sigma_{\text{tri}}$. Note that when the interface fails by chain scission at low Σ , we found 80–90%, not 100%, of dPS on the PS side of the fracture surface, since it is very unlikely that the copolymer chains would always break at the joint between the PS and PVP blocks or in the PVP block itself. Furthermore, Σ^* , or the areal chain density at transition from chain scission to crazeing, is much lower than the transition areal chain density observed for this system.

A self-consistent mean field theory (SCMF) proposed by Shull and Kramer²⁴ that describes the segregation behavior of diblock copolymers at a polymer interface was modified by Dai *et al.*²⁵ in order to determine the segregation character of triblock copolymers. The theory and the segregation experiments suggest that the triblock copolymer chains with short PVP blocks segregating to the interface consist of two chain conformations, staple and tail structures,^{25,26} as depicted in Figure 4b. From SCMF studies, the fraction of staple or tail structure of triblock copolymer can be obtained. Depending on the chain conformation, pull out of the PVP block could occur by single-ended pull out (for the tail structure) or double-ended pull out (for the staple structure) as the interface fractures. The different chain conformations of triblock copolymers will certainly affect the frictional force of the copolymer under pull out. The areal joint density, Σ_{joint} , of a diblock copolymer is equal to its areal chain density, Σ , while that of a triblock copolymer is between Σ (if all chains have a tail conformation) and 2Σ (if all chains have a staple conformation). At the chain pull out to crazeing transition, we can assume that

$$\sigma_{\text{craze}} = \sigma_{\text{pull out}} = f_{\text{mono}} N \Sigma_{\text{joint}}^{\circ} \quad (6)$$

where $\Sigma_{\text{joint}}^{\circ}$ is the areal joint density at transition. It has been previously reported²⁷ that, for a short PVP block being pulled out of PVP homopolymer matrix, the static monomer friction coefficient (f_{mono}) has a value of $\sim 6 \times 10^{-12}$ N/monomer. If the whole triblock copolymer forms a tail structure at the interface, one obtains $\Sigma^{\circ} = \Sigma_{\text{joint}}^{\circ}$ to be 0.1 chains/nm² from eq 6. Similarly, if the whole triblock copolymer forms a staple structure, one obtains $\Sigma^{\circ} = \Sigma_{\text{joint}}^{\circ}/2$ to be 0.05 chains/nm². In fact, we measure Σ° to be about 0.07 chains/nm² both from the $\Sigma(\text{PS})/\Sigma$ data and the G_c measurements. This result thus suggests that there is a mixture of chain conformations of the triblock copolymer at the interface that affects the value of the transition areal joint density. Suppose f is the fraction of tail structure of the triblock at the interface. The transition areal joint density, $\Sigma_{\text{joint}}^{\circ}$, of the triblock copolymer would be equal to $(2(1 - f) + f) \times 0.07$ chains/nm². Substituting the expression of $\Sigma_{\text{joint}}^{\circ}$ into eq 6 and solving for f , we obtain that $\sim 60\%$ of

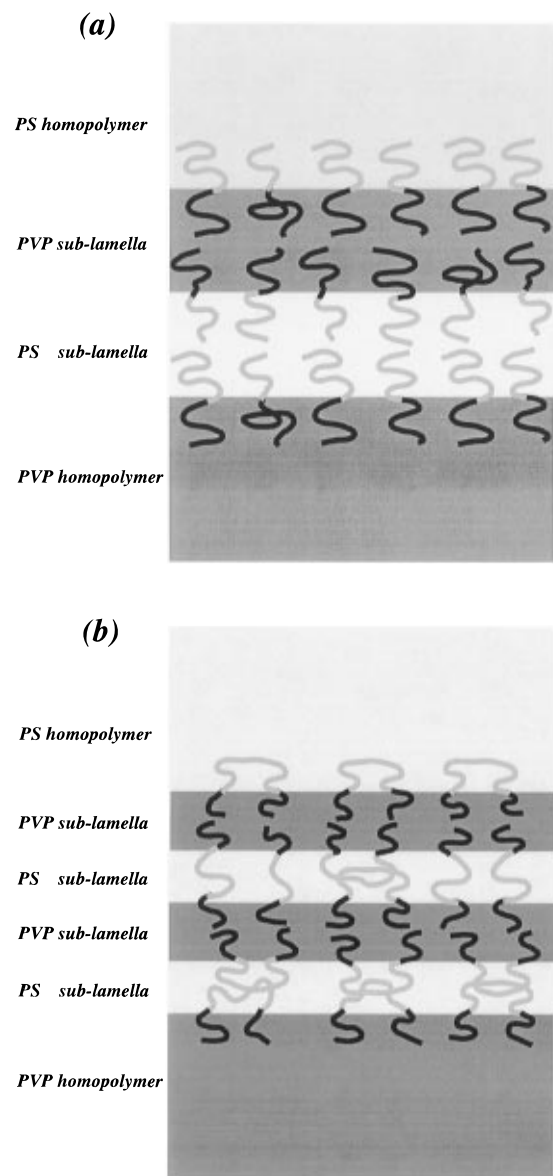


Figure 12. Schematic representation of chain conformation of (a) diblock copolymers and (b) triblock copolymers inside lamellae.

the chains have a tail structure and $\sim 40\%$ of the chains have a staple structure for this triblock copolymer at the interface.

2. Craze Fracture at High Areal Chain Density. Figure 16a shows that, for $\Sigma > 0.07$ chains/nm², the values for fracture toughness rise abruptly to near 30 J/m². Optical microscopy shows craze formation in this high G_c regime. In the high Σ regime, however, the G_c values remain constant while it is expected that G_c should scale with Σ^2 in the crazing regime. This behavior was also observed by Washiyama *et al.*²⁷ for a diblock copolymer of 220–580 PVP-*b*-dPS. As shown in Figure 16b, 40–50% of the total dPS block of the block copolymer was found on the PS side of the fracture surface in the crazing regime, but only 5–10% of dPS of the 540–510 diblock copolymer was found on the PS side when craze breakdown occurred between the block copolymer brush and homopolymer.³ Washiyama *et al.* found that the strength of the craze is weakened by the pull out of the 220–580 diblock copolymer from the PVP side so that the effective areal chain density, Σ_{eff} , of copolymer for supporting crazing at the interface is approximately constant, independent of Σ .

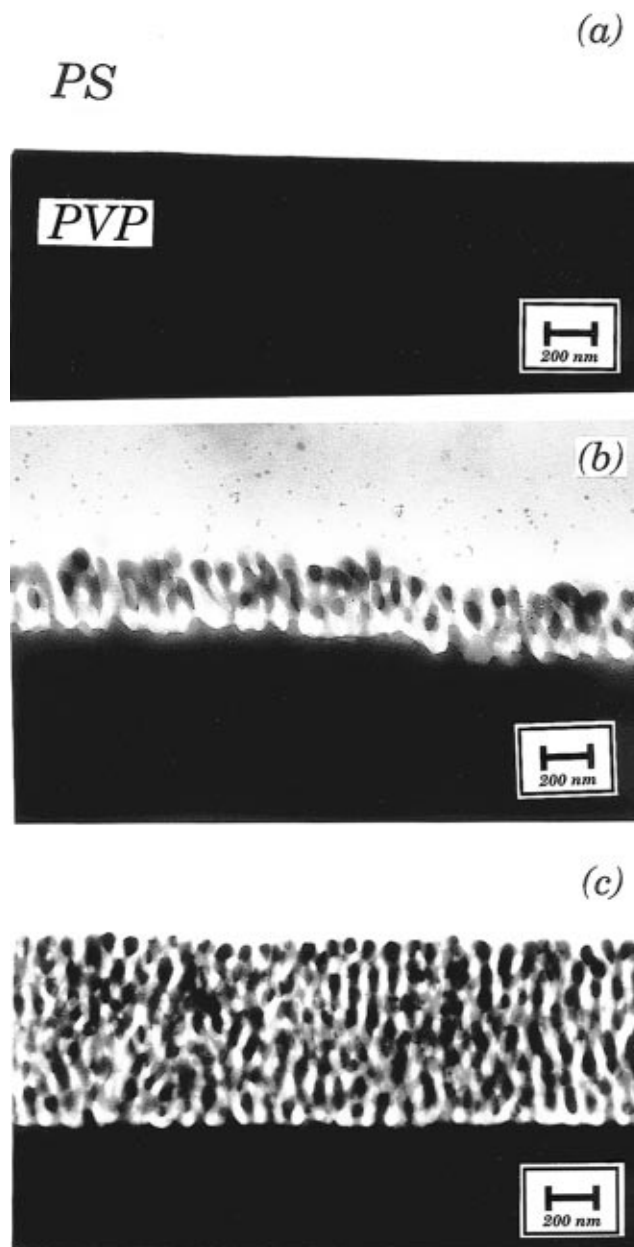


Figure 13. TEM micrographs of the morphology of the 580–1620–580 triblock copolymer microstructure near the interface for (a) $\Sigma = 0.1$, (b) $\Sigma = 0.2$, and (c) $\Sigma > 1.0$ chains/nm².

The plateau G_c values for the triblock copolymer 90–580–90 are larger than those for the corresponding diblock copolymer 220–580 ($G_c \approx 15\text{--}20$ J/m²).²⁷ This modest increase is probably due to two reasons: (1) The presence of the extra 90 units of PVP on the end of 60% of the triblock copolymer chains in the tail conformation gives them an effective length of $580 + 90 = 670$ monomer units in the PS homopolymer versus 580 monomer units for the PVP–dPS diblock copolymer. (2) The dPS block of the 90–580–90 triblock copolymer in the staple conformation has a pseudodiblock copolymer that is longer than the 470 units long dPS block of the 290–470–290 triblock copolymer but much shorter than that of the 580–1620–580 triblock copolymer. In this intermediate block length regime, the pseudodiblock model for entanglement may not be accurate and the 580 unit dPS midblock in the staple conformation may be better entangled than the 580 units dPS block of the 220–580 PVP–dPS diblock copolymer. Experiments

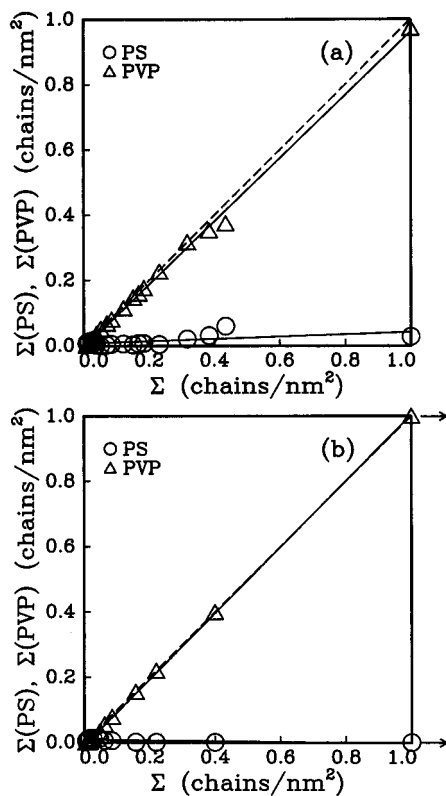


Figure 14. Areal chain density of the dPS block found on the PS (○) or PVP (△) side of the fracture surface as a function of Σ for (a) the 290–470–290 and (b) the 580–1620–580 triblock copolymers.

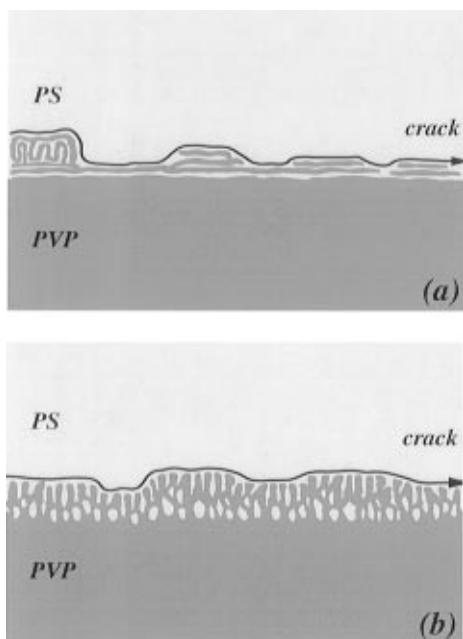


Figure 15. Schematic representation of the crack trajectory near the interface between triblock copolymer layer and homopolymer PS: (a) the 290–470–290 triblock copolymer and (b) the 580–1620–280 triblock copolymer.

using triblock copolymer with a 580 midblock but longer PVP end blocks so that the copolymer would form the staple conformation nearly exclusively at the interface should be able to distinguish between these two possibilities. Further experiments aimed at understanding the effect of the dPS midblock length on the interface reinforcing ability of triblock copolymers also would be useful.

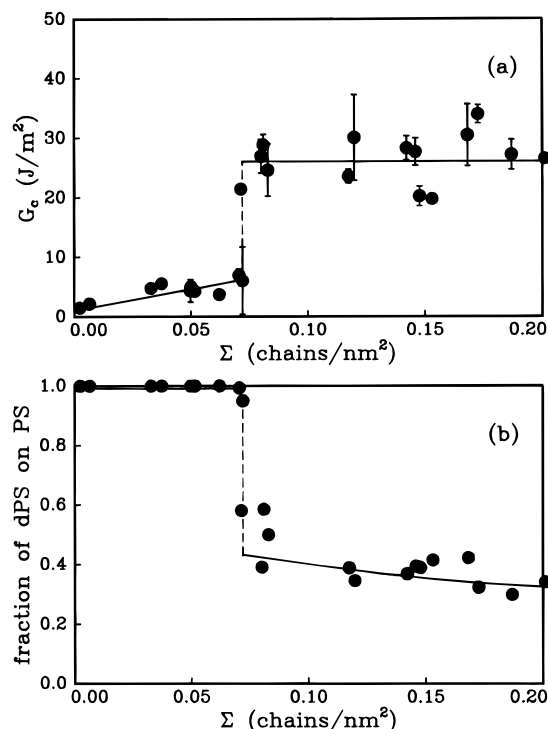


Figure 16. (a) Fracture toughness, G_c , plotted as a function of Σ of the 90–570–90 triblock copolymer. (b) Fraction of the dPS found on the PS fracture surface plotted as a function of Σ .

Conclusions

The addition of PVP-*b*-dPS-*b*-PVP triblock copolymers to the interface between immiscible homopolymers PS and PVP can greatly enhance the fracture toughness of the interface. The strengthening effect and failure mechanisms at the interface strongly depend on the molecular weight of each block, the areal chain density, and the chain conformation of the triblock copolymers at the interface. The results in three main regimes are summarized below.

Regime I ($N_{\text{PVP}} < N_{\text{ePVP}}$). The interface fails by pulling out of the triblock copolymer chains without any significant plastic deformation (G_c is low) at small Σ . At larger Σ , crazing occurs on the PS side of the interface and craze fibrils fail by both chain scission and disentanglement of the dPS block on the PS side and by chain pull out of the PVP blocks from the homopolymer PVP side. Triblock copolymers with short PVP blocks form a mixture of staple and tail structures at the interface.

Regime II ($N_{\text{PVP}} > N_{\text{ePVP}}$ and $\Sigma \leq \Sigma_{\text{sat}}$). There is a fracture mechanism transition from chain scission to crazing for the interface reinforced with triblock copolymers with long PVP blocks. Triblock copolymers with long PVP blocks form a staple structure at the interface. The G_c measurements for $\Sigma \leq \Sigma_{\text{sat}}$ show that a triblock copolymer chain can be treated approximately as two diblock copolymer chains with half the molecular weight in the dPS block of that of the triblock copolymer. The fracture toughness of the interface is controlled not by the areal chain density but by the areal joint density, which takes into account the number of excursions of the triblock copolymers crossing the interface and forming entanglements on both sides of the interface.

Regime III ($N_{\text{PVP}} > N_{\text{ePVP}}$ and $\Sigma > \Sigma_{\text{sat}}$). In this regime, the G_c values of the interface can approach the fracture toughness of the homopolymer PS ($G_c \sim 400$ – 500 J/m^2).²⁸ Large increases in the G_c value are due to

the "bridging chain" structure in the triblock copolymer mesophase enhancing the strength of triblock copolymer domain, which prevents crack propagation through the dPS triblock copolymer layer. In addition, large increases in the G_c come from the fact that the interface between the triblock copolymer layer and the homopolymer PS is roughened as Σ increases. The crack is forced locally to penetrate through homopolymer PS leading to large increases in the fracture toughness.

Acknowledgment. We gratefully acknowledge the support from the Material Science Center (MSC) at Cornell University, which is funded by the National Science Foundation. C.-A. D. was supported in part by the Cornell-Industry Electronic Packaging Alliance Program and by a fellowship from Dow Chemical through the Polymer Outreach Program of the MSC. We also benefited from the use of the Ion Beam Analysis and Electron Microscopy Central Facilities of the MSC at Cornell University and thank J. Hunt, I. Karr, N. Szabo, and P. Revesz of these facilities for their assistance. K.D.J. is grateful for partial financial support in the form of a Feodor-Lynen Fellowship of the Alexander von Humboldt Foundation, Bonn, Germany. We thank C. Daugherty and N. Rizzo from the electron microscopy facility of the College of Agriculture & Life Sciences and Division of Biological Sciences for their help in preparing the microtomed thin sections.

References and Notes

- (1) Fayt, R.; Jérôme, R.; Teyssié, Ph. *J. Polym. Sci., Polym. Phys. Ed.*, **1989**, *27*, 775.
- (2) Brown, H. R. *Macromolecules* **1991**, *24*, 2752.
- (3) Creton, C.; Kramer, E. J.; Hui, C.-Y.; Brown, H. R. *Macromolecules* **1992**, *25*, 3075.
- (4) Hui, C.-Y.; Ruina, A.; Creton, C.; Kramer, E. J. *Macromolecules* **1992**, *25*, 3948.
- (5) Xu, D. B.; Hui, C.-Y.; Kramer, E. J.; Creton, C. *Mech. Mat.* **1991**, *11*, 257.
- (6) Brown, H. R.; Char, K.; Deline, V. R.; Green, P. F. *Macromolecules* **1993**, *26*, 4155.
- (7) Char, K.; Brown, H. R.; Deline, V. R. *Macromolecules* **1993**, *26*, 4164.
- (8) Washiyama, J.; Creton, C.; Kramer, E. J.; Xiao, F.; Hui, C.-Y. *Macromolecules* **1993**, *26*, 6011.
- (9) Creton, C.; Brown, H. R.; Deline, V. R. *Macromolecules* **1994**, *27*, 1774.
- (10) Dai, C.-A.; Dair, B. J.; Dai, K. H.; Ober, C. K.; Kramer, E. J.; Hui, C.-Y.; Jelinski, L. W. *Phys. Rev. Lett.* **1994**, *73*, 2472.
- (11) Tang, W. T.; Hadzioannou, G.; Cotts, P. M.; Smith, B. A.; Frank, C. W. *Polym. Prepr., Am. Chem. Soc., Div. Polym. Chem.* **1986**, *27*(2), 107.
- (12) Mills, P. J.; Green, P. F.; Palmström, C. J.; Mayer, J. W.; Kramer, E. J. *J. Appl. Phys. Lett.* **1984**, *45*, 957.
- (13) Kanninen, M. F. *Int. J. Fract.* **1973**, *9*, 83.
- (14) Xiao, F.; Hui, C.-Y.; Washiyama, J.; Kramer, E. J. *Macromolecules* **1994**, *27*, 4382.
- (15) Washiyama, J.; Creton, C.; Kramer, E. J. *Macromolecules* **1992**, *25*, 4751.
- (16) Odell, J. A.; Keller, A. *J. Polym. Sci., Polym. Phys. Ed.* **1986**, *24*, 1889.
- (17) Kausch, H. H., In *Polymer Fracture*, 2nd ed.; Springer Verlag: Berlin, 1987.
- (18) Brown, H. R., *Macromolecules* **1989**, *22*, 2859.
- (19) Keller, A.; Odell, J. A., In *Processing, Structure and Properties of Block Copolymers*; Folkes, M. J., Ed.; Elsevier: New York, 1985.
- (20) Halperin, A.; Zhulina, E. B. *Europhys. Lett.* **1991**, *16*, 337.
- (21) Matsushita, Y.; Mori, K.; Saguchi, R.; Nakao, Y.; Noda, I.; Nagasawa, M. *Macromolecules* **1990**, *23*, 4313.
- (22) Hadzioannou, G.; Skoulios, A. *Macromolecules* **1982**, *15*, 258.
- (23) Dai, C.-A., Ph.D. Thesis, Cornell University, 1996.
- (24) Shull, K. R.; Kramer, E. J. *Macromolecules* **1991**, *23*, 4769.
- (25) Dai, K. H.; Washiyama, J.; Kramer, E. J. *Macromolecules* **1994**, *27*, 4544.
- (26) The tail structure is not considered in the case of the 290–470–290 and 580–1620–580 triblock copolymers since the PVP block of these triblock copolymers are considerably longer than that of the 90–580–90 triblock copolymer. Contacts between long PVP block with the homopolymer PS (as in the tail structure case) would be very unfavorable since the Flory interaction parameter is large in the PS/PVP system.
- (27) Washiyama, J.; Kramer, E. J.; Hui, C.-Y. *Macromolecules* **1993**, *26*, 2928.
- (28) Benbow, J. J. *Pr. Phys. Soc.* **1961**, *78*, 970.

MA960396S